Grant No. NGR-34-002-175

THE RESISTANCE TO EMBRITTLEMENT BY A HYDROGEN ENVIRONMENT OF SELECTED HIGH STRENGTH IRON-MANGANESE BASE ALLOYS

R. B. Benson, Jr., D. K. Kim,
D. Atteridge, W. W. Gerberich

ABSTRACT

Fe-16Mn and Fe-25Mn base alloys, which had been cold worked to yield strength levels of 201 and 178 KSI, were resistant to degradation of mechanical properties in a one atmosphere hydrogen environment at ambient temperature under the loading conditions employed in this investigation. Transmission electron microscopy established that bands of ε' martensite and fcc mechanical twins were formed throughout the fcc matrix when these alloys were cold worked. In the cold worked alloys a high density of crystal defects were observed associated with both types of strain induced structures, which should contribute significantly to the strengthening of these alloys. High strength iron base alloys can be produced which appear to have some resistance to degradation of mechanical properties in a hydrogen environment under certain conditions.

R. B. Benson, Jr. and D. K. Kim are Associate Professor and Graduate Reserach Assistant, respectively, Materials Engineering Department, North Carolina State University, Raleigh, N. C.; D. Atteridge and W. W. Gerberich are Research Associate and Associate Professor, respectively, Department of Chemical Engineering and Materials Science, University of Minnesota, Minneapolis, Minnesota.

High strength martensitic and ferritic steels are usually embrittled by internal hydrogen[1-5] or a low pressure hydrogen environment[5-7] at substantially reduced stress or stress intensity levels compared to the critical failure levels when hydrogen is not present. The chemistries and microstructures of these alloys are selected to produce high strength, and then the resistance of the alloy to embrittlement by hydrogen is determined. If a hydrogen environment affects the mechanical properties of an austenitic steel, usually the ductility is decreased with only a slight decrease in strength level, if any at all[8-14]. However, severe electrolytic charging[15-18] or thermal charging in a high pressure hydrogen environment can decrease the ductility of many austenitic steels[12,19,20]. By investigating the relationship of alloy chemistry and metallurgical microstructure to hydrogen assisted cracking in simple alloy systems with a face centered cubic matrix, it may be possible to design high strength alloys which have some resistance to the degradation of mechanical properties in a hydrogen environment under certain conditions.

Certain iron base and cobalt base fcc alloys exhibit high work hardening rates and can be cold worked to high strength levels[21-25]. When the microstructures of these alloys have been studied, it has been observed that these effects are due either to mechanical twinning or strain induced martensite[21-24,26,27]. For Fe-Cr-Ni base austenitic alloys in which strain induced or chemical transformations occur usually when a hcp martensite is formed, a bcc martensite is also formed[26,28-32]. In

Fe-Mn base alloys for certain ranges of alloy chemistries the phases observed have been only fcc and hcp[21,33-35].

If substantial amounts of α'-bcc martensite form in an alloy with an austenitic matrix during mechanical testing, it has been observed that a hydrogen environment can degrade the mechanical properties of the alloy even at a pressure of one atmosphere for some alloys[9,36-38]. The ductility of low stacking fault energy (SFE) austenitic steels, some of which are stable with respect to formation of α', can be reduced in the presence of hydrogen[12,14]. High energy rate forging (HERF) forms dislocation tangles in austenitic alloys of this type and results in only a slight degradation of the ductility of the alloys in the presence of hydrogen as compared to an inert environment[12]. Cold working low SFE austenitic alloys in which substantial amounts of ε' and/or fcc mechanical twins form along with a relatively high concentration of dislocations may produce a high strength alloy which has some resistance to degradation of mechanical properties in a hydrogen environment.

A Co-Fe base alloy which is fcc in the solution treated state can be cold worked to a yield strength level of 240 KSI and is partially strengthened by the formation of ε'-hcp martensite and fcc mechanical twins[24]. This alloy at a yield strength level of 240 KSI did not appear to be degraded when loaded in a one atmosphere hydrogen environment at ambient temperature[24]. An Fe-25Mn base alloy similar to the one used in this investigation was severely hot worked at 400°C to a yield strength level of 179 KSI in order to suppress a martensitic transformation and produce an alloy that might transform to ε' martensite when plastically deformed at ambient temperature. The mechanical properties of this alloy

were not affected in a one atmosphere hydrogen environment at ambient temperature, and x-ray analysis indicated the presence of some ε'[39]. However, the mechanical properties of several other hot worked Fe-Mn-C alloys with less manganese were affected by a hydrogen environment[39].

In Fe-Mn base alloys, a variety of phases can be present at ambient temperature ranging from various bcc phases in dilute alloys through epsilon and austenite in the alloys with higher manganese concentrations[21,33-35,40-42]. Only epsilon and austenite have been reported to be present for certain higher manganese concentration ranges[21,33-35]. For binary Fe-Mn alloys it has been shown that for manganese concentrations greater than ten percent the free energy of formation of epsilon in austenite becomes less than for bcc phases[35]. Since carbon in solid solution is a potent austenitic stabilizing element, the addition of carbon to Fe-Mn binary alloys will stabilize the alloy with respect to martensitic transformations[21]. In Hadfield steels which contain about 13% Mn and 1.0% C, fcc mechanical twins are formed when the alloy is plastically deformed which are responsible for the high rate of work hardening[22]. Consequently, when a substantial amount of either a strain induced martensitic transformation or mechanical twinning occurs in an austenitic Fe-Mn base alloy during plastic deformation, the alloy will exhibit a high work hardening rate and can be cold worked to produce high yield strength levels[21,22].

The objective of this investigation was to study the effect of a hydrogen environment on the fracture behavior of selected Fe-Mn base

alloys which were cold worked to produce high yield strength levels. On the basis of available information, alloys were selected in which it was thought cold work would produce either strain induced ε'-hcp martensite or mechanical twinning in an fcc matrix. The initial microstructure of each alloy in both the solution treated and initial cold worked states was determined using transmission electron microscopy techniques in conjunction with x-ray analysis and optical microscopy.

EXPERIMENTAL PROCEDURE

An Fe-Mn base alloy containing twenty-five percent manganese with 0.29 percent carbon was selected for it was thought that cold working of this alloy would produce strain induced ε'-martensite in an fcc matrix. This alloy was cold worked thirty percent before mechanical testing. On the basis of microstructural studies of cold worked Hadfield steels[22] the alloy cryogenic Tenelon (i.e. Fe-16Mn alloy) was selected in which cold working might produce primarily mechanical twinning in the austenitic matrix[43]. It has been reported that a similar alloy can be cold worked to yield strength levels greater than 200 KSI[25]. For an alloy with a chemical composition similar to the Fe-16Mn alloy of this investigation, magnetization measurements indicated the presence of less than one percent of a magnetic bcc phase after severe plastic deformation[43]. The alloys were solution treated at 1125°C. The chemical composition of these alloys is presented in Table I.

Single edge notch specimens (SEN), for which a stress intensity calibration is available[44], and tensile specimens were used to determine

the fracture behavior of the alloys. The width of the SEN specimens was one inch with a thickness of 0.056 inch for the Fe-25Mn alloy and of 0.040 inch for the cryogenic Tenelon. All the SEN specimens were precracked by fatigue loading prior to loading in tension with the specimens which were tested in hydrogen being precracked in this environment just prior to tensile testing. The maximum stress intensity parameter in air was determined for each alloy. The tests in a hydrogen environment were run at 0.9 of an atmosphere and at ambient temperature. The SEN specimens were held at constant increasing successive stress intensity levels, and the crack growth rate was monitored. The SEN specimens were tested in a stainless steel high vacuum chamber mounted on a standard MTS test system. The tensile tests were run at a strain rate of 5×10^{-4} IN/IN in a stainless steel vacuum chamber mounted on a tensile machine. The test chambers were evacuated and flushed with hydrogen before the hydrogen test environment was introduced. High purity hydrogen which was passed through a liquid nitrogen trap was used for a test environment.

X-ray analysis was carried out using a diffractometer with Mo Kα radiation. Optical microscopy[34,43] and transmission electron microscopy (TEM) specimens[27,45] were prepared using techniques that have been described elsewhere. The TEM specimens were examined in a JEM-7A transmission electron microscope operated at 120 KV and equipped with a goniometer 30° tilt stage. Electron fractographs were obtained from a JSM-2 scanning electron microscope.

RESULTS

The mechanical properties of the alloys are given in Table II. Cold working of these Fe-Mn base alloys can produce high yield strength levels of the order of 200 KSI. The maximum stress intensity levels listed in the table are the levels at which the alloy fractured in either an air or hydrogen environment. From the stress intensity values, crack growth rates and ductility data listed in Table II, it appears that the mechanical properties of neither of the alloys was degraded by a hydrogen environment under the test conditions employed. Comparison of the fracture modes for specimens of the same alloy using the scanning electron microscope revealed similar fracture modes in both the air and hydrogen environments. Therefore, high strength iron-manganese base alloys can be produced which appear to be resistant to degradation of mechanical properties in a one atmosphere hydrogen environment at ambient temperature under the loading conditions employed in this investigation.

For the Fe-16Mn and Fe-25Mn alloys of this study magnetization measurements indicated the presence of less than one percent of a magnetic phase in the as received cold worked alloys from which the mechanical test specimens were obtained and in specimens taken from the gage section of fractured tensile specimens. The initial microstructure of each alloy in both the solution treated and cold worked states was investigated using primarily transmission electron microscopy techniques in conjunction with x-ray and optical microscopy techniques in order to correlate the mechanical properties with the initial metallurgical microstructure. X-ray analysis of the solution treated Fe-16Mn alloy

revealed only the fcc matrix structure. Transmission electron microscopy analysis revealed only traces of other structures for the alloy in this state. Specimens of this alloy which were cold rolled twenty and fifty percent respectively were examined. X-ray analysis did not reveal any evidence of a phase other than fcc in the cold worked specimens. Optical micrographs of the deformed alloys revealed a deformed grain structure with a uniform complex fine structure in the matrix, Figure 1. Transmission electron microscopy revealed that the predominant strain induced transformation was the formation of fcc mechanical twins in the fcc matrix although some strain induced ε'-hcp martensite was observed. A bright field transmission electron micrograph of a single fcc mechanical twin variant (111) is shown in Figure 2a for a specimen cold worked twenty percent. A selected area electron diffraction pattern from this region, Figure 2b, reveals the fcc matrix orientation is $[411]_\gamma$ with a $[011]_T$ twin orientation; and the individual diffracted beams of each structure are indexed in Figure 2c. The orientation relations between fcc matrix zones and fcc twin zones were obtained from stereographic analysis on the basis of four possible twin variants which form on {111} matrix planes. The reversal of contrast for the band structure between the bright field image of Figure 2a and the dark field image of Figure 2d, using the $(1\bar{1}1)_T$ beam from the twin pattern, proves that the bands are fcc mechanical twins since when a beam diffracted from the twin structure is used to form the image the twins appear bright in relation to the fcc matrix. In Figure 2d, dislocations and sharp changes of contrast can be

observed along the twins. A dark field image formed from the superimposed $(2\bar{2}0)_\gamma$ - $(02\bar{2})_T$ beams, Figure 2e, reveals a high density of dislocations associated with the twin bands. These may be mostly matrix-twin interface dislocations which in general it has been shown must be generated for dislocations to move through a twinned crystal[22]. The greater the density of twins and the density of dislocations associated with twins, the higher is the applied stress necessary for dislocation motion. As is illustrated in Figure 2e, an alloy cold worked twenty percent has a relatively high density of both twins and of dislocations associated with the twins which would help account for the high yield strength levels produced by cold working this alloy. Many regions of this specimen also contained more than one twin variant.

There are two twin variants in the bright field micrograph from an Fe-16Mn specimen cold worked fifty percent, Figure 3a. An analysis of the selected area diffraction pattern from this region, assuming that the observed bands were fcc mechanical twins formed on the {111} matrix planes, resulted in a correlation between the observed diffraction pattern, Figure 3b, and the calculated pattern, Figure 3c. The matrix orientation was $[125]_\gamma$ with $[110]_T$ and $[1\bar{2}\bar{1}]_T$ twin orientations which correspond to twin plane variants (111) and $(1\bar{1}1)$ respectively. The (111) twin variant is revealed by a dark field image with the $(00\bar{2})_T$ twin beam from the $[110]_T$ twin pattern, Figure 3d. A dark field image with the $(11\bar{1})_T$ twin beam from the $[1\bar{2}\bar{1}]_T$ twin pattern illustrates the $(1\bar{1}1)$ twin variant, Figure 3e. Trace analysis showed that the twin planes were

along $\{111\}_\gamma$. There is a dense irregular arrangement of dislocations in the fcc matrix, Figure 3a.

Two epsilon variants are observed in the bright field micrograph of Figure 4a obtained from a Fe-16Mn alloy cold worked twenty percent. An analysis of a selected area diffraction pattern from this region, Figure 4b, revealed a $[015]_\gamma$ matrix orientation with $[0\bar{1}11]_{\varepsilon'}$ and $[\bar{1}01\bar{1}]_{\varepsilon'}$ orientations which correspond to an ε' variant forming on the $(\bar{1}11)_\gamma$ plane and an ε' variant forming on the $(11\bar{1})_\gamma$ plane, Figure 4c. The two variants are illustrated by dark field images formed with the $(10\bar{1}1)_{\varepsilon'}$ beam, Figure 4d, and with the $(1\bar{1}0\bar{1})_{\varepsilon'}$ beam, Figure 4e. A high density of dislocations and fault structures is observed to be associated with the ε' bands of Figure 4d, and Figure 4f, which is from a region adjacent to the region of Figure 4a. This high density of defects associated with the ε' bands should contribute significantly to the strengthening of a cold worked alloy which contains thin bands of ε'-martensite.

X-ray analysis of the Fe-25Mn alloy revealed only a trace of ε and no α in the solution treated alloy and a substantial amount of ε' with no α' in the alloy cold worked thirty percent. An optical micrograph of the cold worked alloy reveals severe deformation and a fine deformation structure, Figure 5. A region from a Fe-25Mn alloy cold worked 30% is illustrated in the bright field electron micrograph of Figure 6a. A selected area diffraction pattern from region A, Figure 6b, reveals a $[110]_\gamma$ matrix orientation, a $[\bar{1}\bar{1}0]_T$ fcc twin orientation, and a $[1\bar{2}10]_{\varepsilon'}$ orientation as illustrated in the diagram of Figure 6c. The band structures contained in the fcc matrix are revealed by the dark field

image from a $(002)_\gamma$ beam, Figure 6d. The ε' phase from the $(1\bar{1}1)$ variant is observed when the $(10\bar{1}1)_{\varepsilon'}$ beam is used to form a dark field image, Figure 6e. An image with the $(1\bar{1}\bar{1})_T$ twin beam reveals the $(1\bar{1}1)$ fcc twin variant, Figure 6f. A selected area diffraction pattern from region B tilted to the $[0\bar{1}11]_{\varepsilon'}$ orientation reveals the presence of a second epsilon variant of the type (111) present in the matrix. A dark field image with the $(10\bar{1}1)_{\varepsilon'}$ beam from the $[0\bar{1}11]_{\varepsilon'}$ zone illustrates the second ε' variant, Figure 6g. The predominant strain induced structure in the Fe-25Mn alloy is epsilon martensite. A dense irregular arrangement of dislocations is observed in the fcc matrix, Figure 6a.

DISCUSSION

The high strength cold worked Fe-Mn base alloys studied in this investigation were partially strengthened by the formation of strain induced ε'-hcp martensite and fcc mechanical twins in an austenitic matrix. The predominant strain induced strengthening structures were mechanical twins in the Fe-16Mn alloy and epsilon martensite in the Fe-25Mn alloy. At yield strength levels of 178-201 KSI, the mechanical properties of these alloys did not appear to be affected by a one atmosphere hydrogen environment at ambient temperature under the loading conditions employed in this investigation.

A series of Fe-Mn-C alloys containing approximately 0.3% C with 16, 20 and 25% Mn respectively, were hot worked to yield strength levels in the range of 173 to 193 KSI[39]. During mechanical testing in a one atmosphere hydrogen environment at ambient temperature, the ductility of only the Fe-16Mn and Fe-20Mn alloys was decreased; and slow crack growth was observed for the Fe-16Mn alloy only. After mechanical testing,

the Fe-20Mn and Fe-25Mn alloys were reported to contain austenite and ε martensite; and the Fe-16Mn alloy contained these phases plus α' martensite.

The effect of hydrogen on the mechanical properties of an alloy should depend on the alloy chemistry, metallurgical microstructure, and test conditions with respect to hydrogen. The hydrogen test conditions would be determined by the pressure and temperature of a hydrogen test environment or the degree of saturation of an internally charged alloy at a given test temperature. When a substantial amount of α'-bcc martensite forms during mechanical testing of an austenitic steel, a hydrogen environment can degrade the mechanical properties of the alloy even at pressure of one atmosphere for some alloys[9,36-38]. In the presence of hydrogen the ductility of austenitic steels, some of which are stable with respect to formation of α', has been observed to be related to the degree of coplanar slip in the alloy which is a function of the stacking fault energy[12,14]. In general, the ductility of low SFE austenitic alloys appears to be reduced during tensile tests in a high pressure hydrogen environment while the ductility of high SFE alloys appears not to be or only slightly affected[12,14]. If enough hydrogen is introduced into austenitic steels, usually by severe electrolytic charging[15-18] or charging at an elevated temperature in a high pressure hydrogen environment[12,19,20], the ductility of many austenitic alloys can be reduced. The greater decrease in ductility due to the presence of hydrogen in alloys with coplanar slip has been interpreted in terms of the transport of hydrogen with moving dislocations to points where

microcracks or microvoids nucleate[12,14]. For an alloy in which coplanar slip occurs, it has been proposed that the moving dislocations will tend to release hydrogen to form molecular hydrogen at microcracks and microvoids which will stabilize and aid in the growth of these defects; in higher SFE alloys where cross slip readily occurs, moving dislocations will tend to bypass dislocation barriers. The alloys of this investigation in which strain induced ϵ' and fcc mechanical twins form are low SFE alloys which exhibit coplanar slip in the low strength states. Tensile tests in a 10^4 PSI hydrogen environment at ambient temperature with a solution treated Fe-16Mn alloy similar to the one used in this investigation have revealed somewhat of a decrease in ductility although the yield and ultimate strengths did not decrease[12]. High energy rate forging (HERF) of a low and an intermediate SFE alloy produced a major improvement in the ductility of the alloys in the presence of hydrogen in comparison to the same alloys with no exposure to hydrogen[12]. This change in mechanical properties was attributed to an observed change of dislocation structure from a coplanar type in the solution treated alloys to a tangled type in the HERF alloys. The ductility of a low stacking fault energy Fe-Cr-Ni base austenitic alloy in the cold worked and solution treated states in contact with lithium hydride was not decreased while the ducility of the alloy in the solution treated state with a machined surface was decreased under the same test conditions[14]. These and other results with this alloy were interpreted in terms of the number of moving dislocations available to transport hydrogen into the metal and the mean free path for moving dislocations[14].

In the heavily cold worked alloy it was proposed that there were many sources of mobile dislocations, but the mean free path of mobile dislocations was too short for a substantial amount of transport of hydrogen from the surface.

The microstructures of the cold worked alloys employed in this study consist of relatively closely spaced regions of strain induced ε' or fcc mechanical twins with a dense irregular arrangement of dislocations in the fcc matrix. A substantial number of defects are also associated with the strain induced structures. This microstructure should severely limit the mean free path of moving dislocations and thereby could inhibit the transport of hydrogen from the surface. This type of microstructure should also inhibit coplanar dislocation motion and the formation of dislocation pileups. In order to more fully evaluate the relationship between metallurgical microstructure and the resistance to degradation of mechanical properties by hydrogen for the alloys employed in this investigation, it will be necessary to study the alloys in various metallurgical states under more severe test conditions with respect to hydrogen.

Thermodynamic and kinetic factors can also play an important role with respect to the effect of a hydrogen environment on the mechanical properties of alloys. The severity of the test conditions with respect to hydrogen could be an important factor in the present investigation. Several recent papers have discussed in detail the processes involved in transporting hydrogen from a gaseous environment to some interior point in a metal and have stressed that these processes could control

whether a hydrogen environment affects the mechanical properties of an alloy under a particular set of test conditions[7,12-14,46,47]. These processes include several surface reactions[7,12-14,46,47], diffusion of hydrogen[7,13,46,47], transport of hydrogen with moving dislocations[12,14], and any reactions that occur in the metal[7,12-14,46,47]. Temperature and pressure may have a strong effect on these processes. It is known that the diffusivity of hydrogen in fcc iron structures such as austenite is several orders of magnitude slower than in the bcc phase[48,49]. Thus, it may be that the high strength alloys employed in this investigation could be affected if higher temperatures and hence higher diffusivities were involved. This suggests additional experiments at elevated temperatures for delineating the character of the hydrogen interaction at a crack tip in fcc structures.

High strength steels are designed by selecting microstructures which will produce high strength and these have usually been alloys that contained bcc or bct phases. Consequently, high strength steels have been embrittled by a low pressure hydrogen environment[5-7]. The hydrogen embrittlement of alloys should be a function of both alloy chemistry and microstructure. It may be possible by studying the effect of hydrogen on alloys with different chemistries and simple well characterized microstructures to design alloys which have some resistance to degradation of mechanical properties by a hydrogen environment under certain conditions. This investigation has established that the mechanical properties of certain high strength iron base alloys with specific microstructures do not appear to be degraded by a hydrogen

environment under the test conditions employed. A Co-Fe base alloy cold worked to a yield strength level of 240 KSI, which was partially strengthened by the formation of strain induced ε'-hcp martensite and fcc mechanical twins in a fcc matrix, also did not appear to be degraded in a one atmosphere hydrogen environment[24].

In order to select Fe-Mn base alloys which may be partially strengthened by the formation of strain induced ε'-hcp martensite or fcc mechanical twins in a fcc matrix, information is required which correlates alloy chemistry to the structures present in various metallurgical states. There have been several investigations in Fe-Mn binary and Fe-Mn-C ternary systems which correlate the alloy chemistry with the phases present after various types of heat treatment and cold working[21,33-35,41]. Some work has also been done in developing more complex austenitic Fe-Mn base alloys, one of which was employed in this investigation[22,25,43,50]. The microstructures produced in these more complex alloys by cold work have often not been completely determined, but the high yield strength levels that can be obtained by cold work suggest the presence of strain induced transformations. In fcc crystals ε' martensite is produced when stacking faults form on alternate (111) planes and fcc mechanical twins are formed by faulting on consecutive (111) planes[51]. There is direct evidence to indicate that ε' martensite is produced by the formation of stacking faults on alternate slip planes in bundles of irregularly spaced stacking faults in an fcc matrix[52]. Therefore, a decrease in stacking fault energy in a fcc

matrix should increase the tendency to form strain induced ε' martensite or fcc mechanical twins[22].

The concept of grain refinement has been employed to help explain the rapid rate of work hardening and the high strength levels produced in cold worked alloys by the formation of strain induced structures[22,53]. The Petch correlation[54], which was developed to explain the yield strength dependence on grain size, has been found to correlate reasonably well the increase in yield strength with the average decrease in spacing between ε' bands in an alloy that was strengthened by the formation of thin ε' bands in an fcc matrix[53]. For a material containing bands of another structure in the matrix to deform plastically, there must be some mechanism for transmitting plastic deformation through the bands. For the general case of fcc mechanical twins in a fcc matrix it has been shown that this occurs by the dissociation of a matrix slip dislocation at a matrix-twin interface to form an interface dislocation and a slip dislocation in the twin crystal[22]. The high concentration of dislocations observed associated with the mechanical twins in this investigation may be primarily these interface dislocations. However, it is clear that the high density of dislocations associated with the twins should make it more difficult to move dislocations through the crystal and therefore should strengthen the crystal significantly. In a highly deformed fcc crystal containing ε' bands, a high density of defects associated with the ε' bands was also observed. Therefore, it appears that mechanical twins or ε'-hcp martensitic bands in a heavily cold

worked fcc matrix will have a high density of defects which should significantly strengthen the material.

This investigation has established that certain Fe-Mn base alloys, with specific chemistries, which have been cold worked to produce high yield strengths appear to be resistant to degradation of mechanical properties by a one atmosphere hydrogen environment at ambient temperature under the loading conditions employed in this investigation. These alloys were partially strengthened by the formation of strain induced fcc mechanical twins and ε'-hcp martensite in the fcc matrix. These results help to establish that alloy chemistry and metallurgical microstructure can play an important role with respect to the effect of a hydrogen environment on the mechanical properties of alloys.

ACKNOWLEDGEMENT

This work was supported by NASA Ames Research Center under grant No. NGR 34-002-175. The encouragement of D. P. Williams of that organization is especially appreciated. The authors wish to thank R. A. McCoy for his assistance and J. G. Donelson of the United States Steel Corporation for providing the alloy cryogenic Tenelon.

TABLE I

Chemical Composition of Alloys in Weight Percent

Alloy	Fe	Mn	C	N	Cr	Ni
Fe-16Mn	Bal.	15.9	0.08	0.40	18.0	5.5
Fe-25Mn	Bal.	25.2	0.29			

TABLE II

Mechanical Properties of Alloys

Specimen	Environment	Yield Strength (KSI)	Red. in Area (%)	Total Elongation (%)	K_I (KSI-IN$^{1/2}$)	Crack Growth Rate (IN/MIN)
Fe-16Mn	A	202	32	4.9	96(M)	--
C.W. 50%	H_2	200	35	5.1	89	Nil
	H_2				98(M)	
Fe-25Mn	A	177	14	2.3	96(M)	--
C.W. 30%	H_2	179	13	1.8	78	Nil
	H_2				86	Nil
	H_2				93(M)	--

Notes: (1) K_I(M) = maximum K_I calculated from load at fracture.
(2) Tests at ambient temperature.

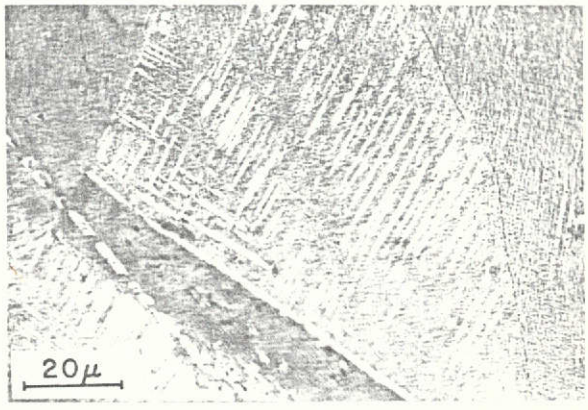

(a)

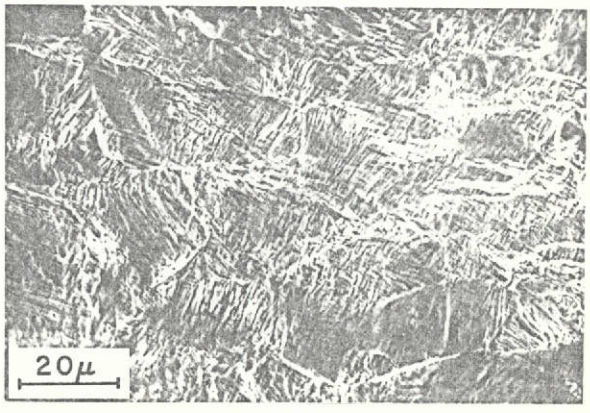

(b)

Figure 1. Plastically deformed Fe-16Mn alloy (a) 20%, (b) 50%.

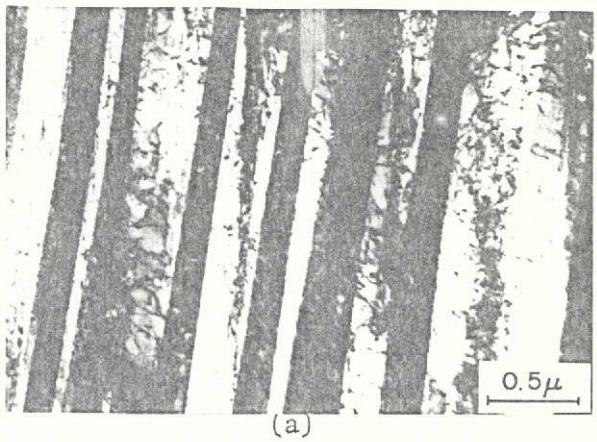

(a)

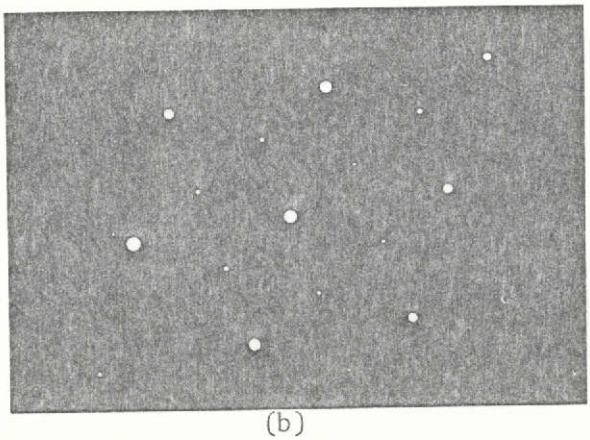

(b)

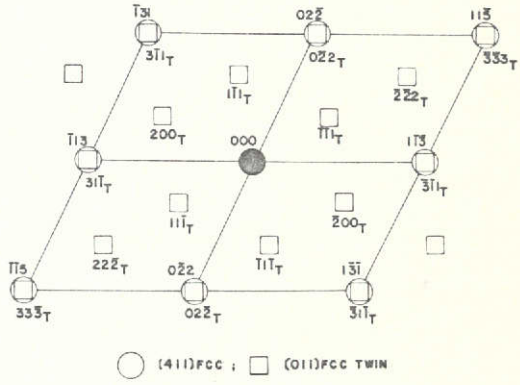

(c)

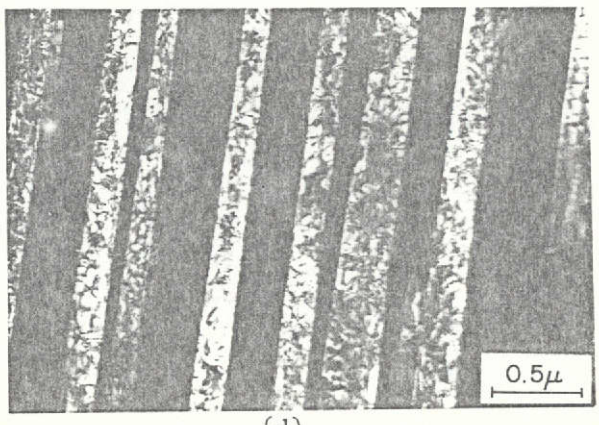

(d)

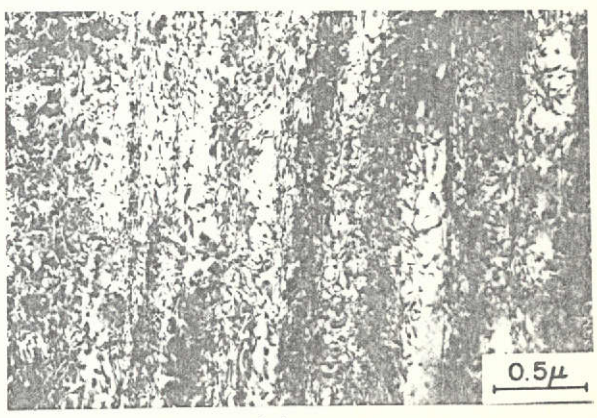

(e)

Figure 2. Deformation twins in an Fe-16Mn alloy deformed 20%. (a) Bright field electron micrograph; (b) Selected area diffraction pattern; (c) Indexed pattern - the pattern consists of two superimposed reciprocal lattice sections $[411]_\gamma$, $[011]_T$ γ twin; (d) Dark field micrograph of the (111) twin variant with $(1\bar{1}1)_T$ twin beam; (e) Dark field micrograph with $(0\bar{2}2)_\gamma$ - $(02\bar{2})_T$ superimposed beams showing dislocations associated with twin bands.

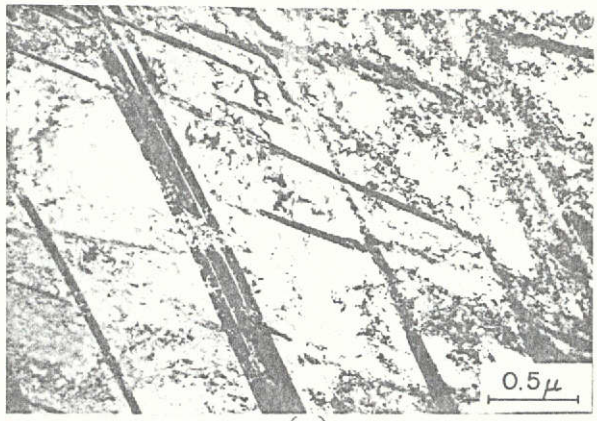

(a)

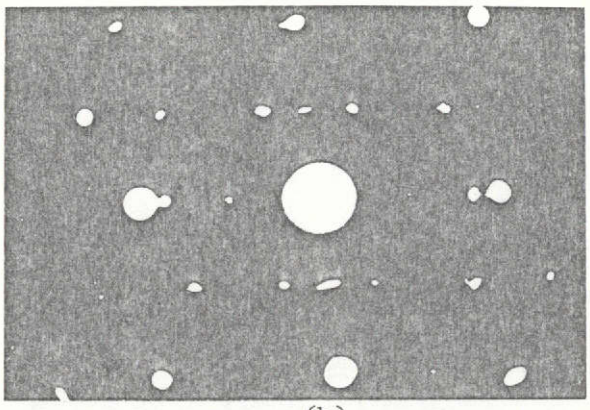

(b)

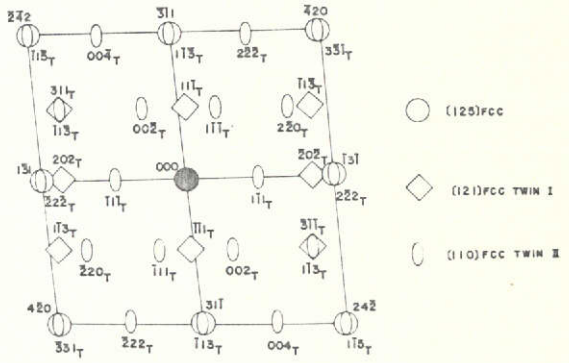

(c)

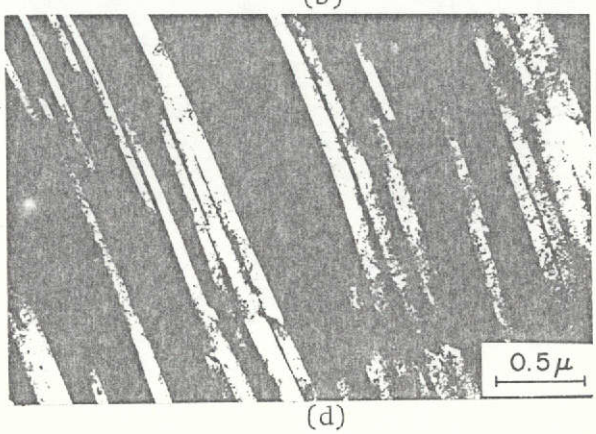

(d)

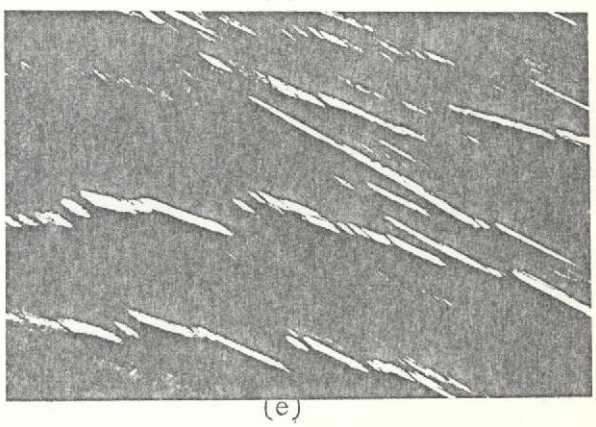

(e)

Figure 3. Two deformation twin variants in an Fe-16Mn alloy deformed 50%. (a) Bright field electron micrograph; (b) Selected area diffraction pattern; (c) Indexed pattern - the pattern consists of three superimposed reciprocal lattice sections $[125]_{\gamma}$, $[1\bar{2}\bar{1}]_{T}$ twin I, $[110]_{T}$ twin II; (d) Dark field micrograph of the (111) twin variant with $(00\bar{2})_{TII}$ twin beam; (e) Dark field micrograph of the $(1\bar{1}\bar{1})$ twin variant with $(11\bar{1})_{TI}$ twin beam.

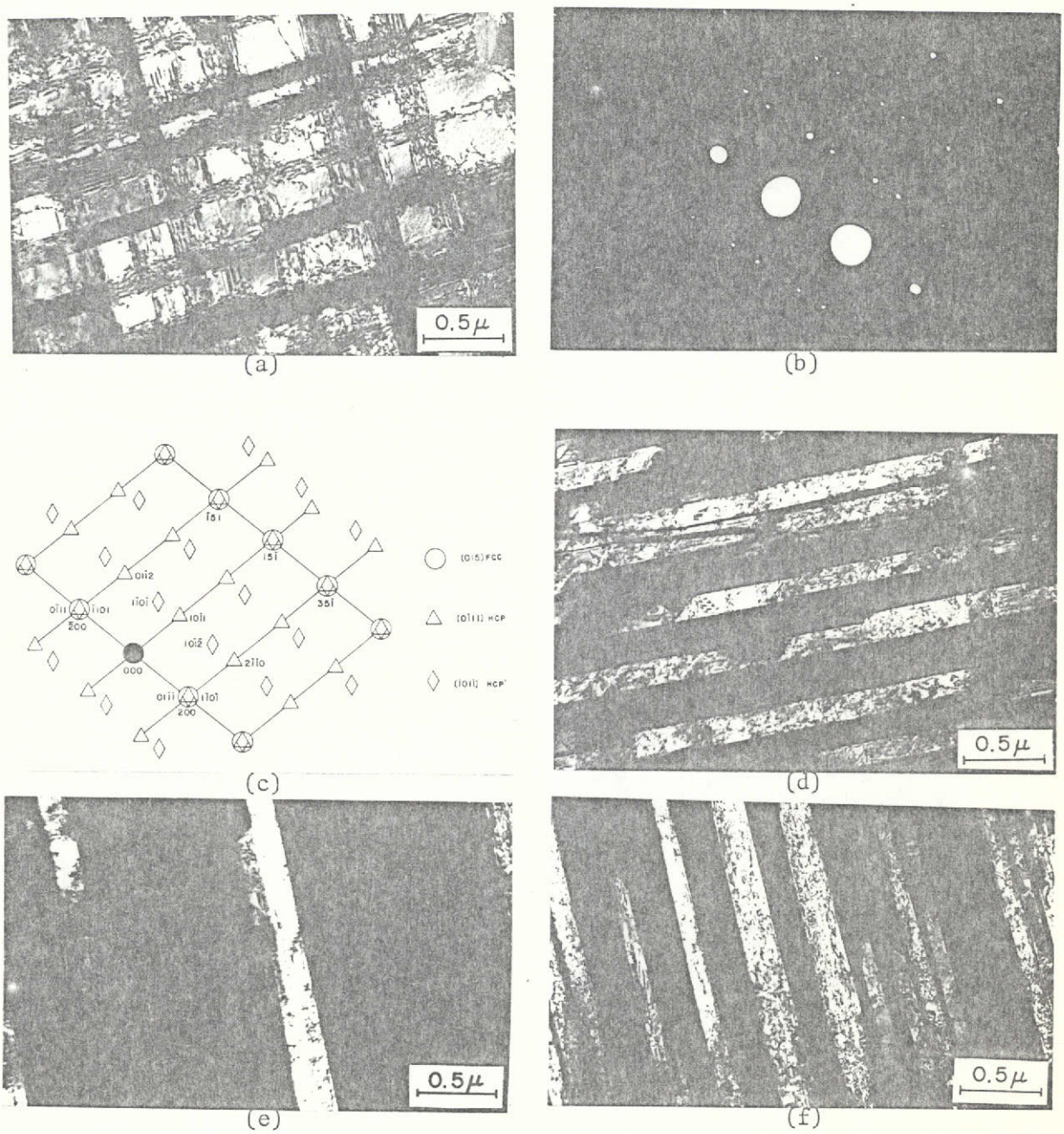

Figure 4. Epsilon variants in an Fe-16Mn alloy deformed 20%. (a) Bright field electron micrograph; (b) Selected area diffraction pattern; (c) Indexed pattern - the pattern consists of three superimposed reciprocal lattice sections $[015]_\gamma$, $[0\bar{1}11]_\varepsilon$, $[\bar{1}01\bar{1}]_\varepsilon$,; (d) Dark field micrograph of the $(\bar{1}11)_\varepsilon$ variant with the $(10\bar{1}1)_\varepsilon$ beam; (e) Dark field micrograph of the $(11\bar{1})_\varepsilon$, variant with the $(1\bar{1}0\bar{1})_\varepsilon$, beam; (f) Dark field micrograph of $(11\bar{1})_\varepsilon$, variant with the $(1\bar{1}0\bar{1})_\varepsilon$, beam.

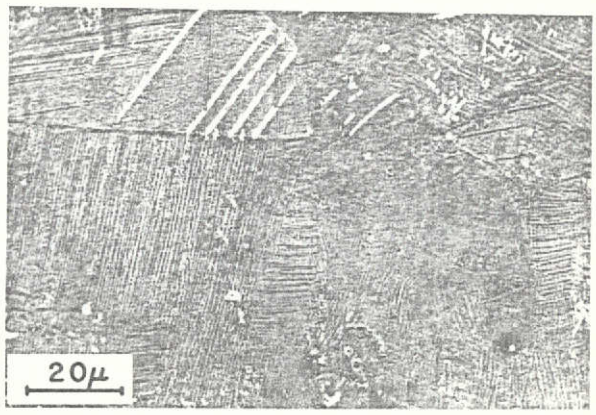

Figure 5. Optical micrograph of Fe-25 Mn alloy deformed 30%.

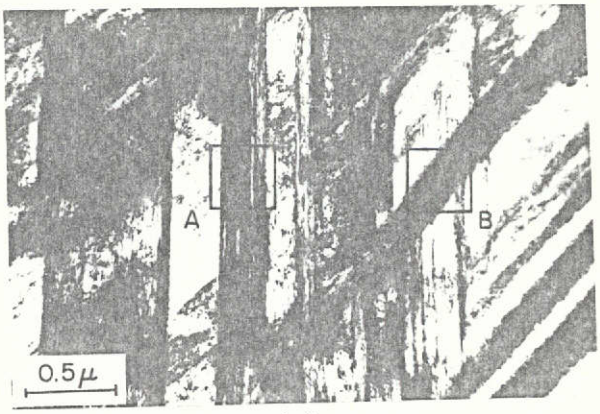

(a)

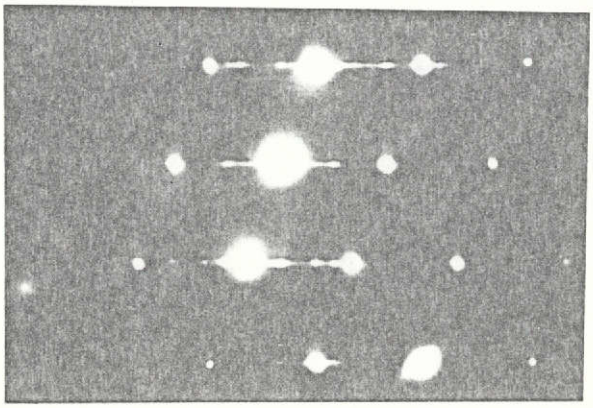

(b)

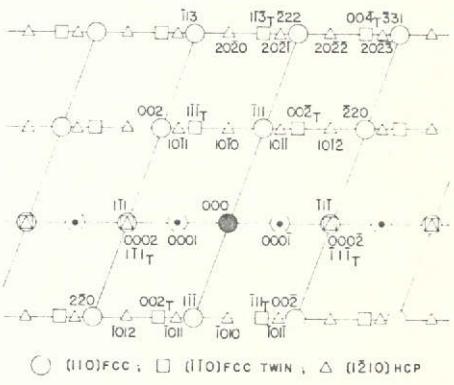

(c)

Figure 6. Typical region in an Fe-25 Mn alloy deformed 30%.
(a) Bright field electron micrograph.
(b) Selected area diffraction pattern from region A.
(c) Indexed pattern from region A - the pattern consists of three superimposed reciprocal lattice sections $[110]_{\gamma}$, $[1\bar{2}102]_{\varepsilon}$, and $[\bar{1}\bar{1}0]_{T}$ twin.

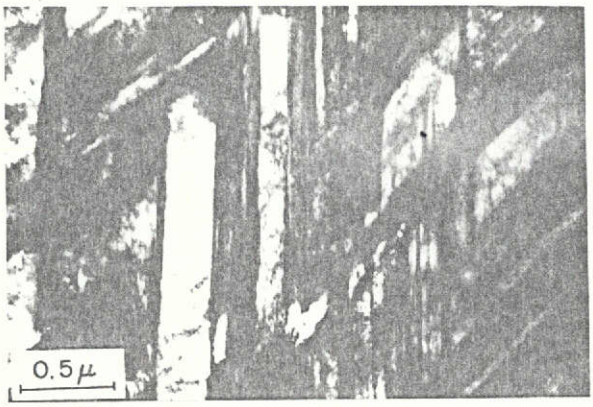

(d)

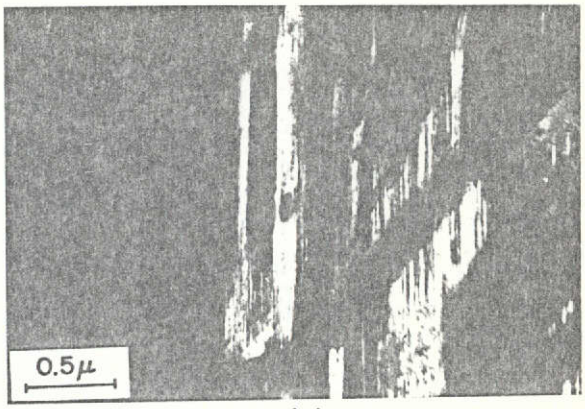

(e)

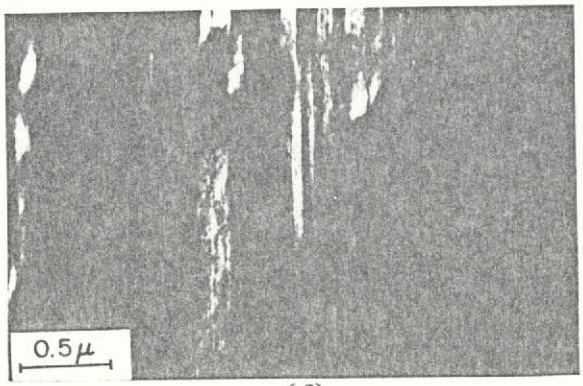

(f)

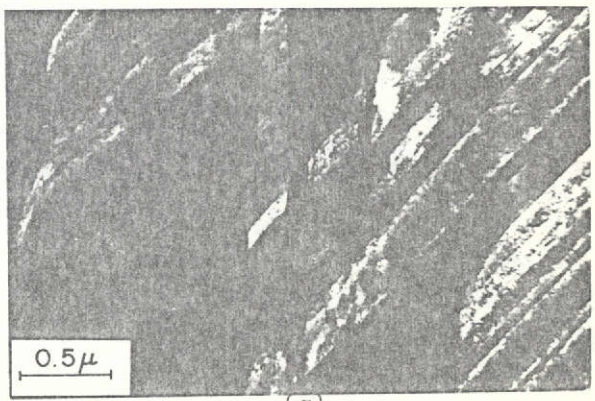

(g)

Figure 6 - continued.

(d) Dark field image with $(002)_\gamma$ beam illustrating the band structure.

(e) Dark field image of the $(1\bar{1}1)$ ε variant with $(10\bar{1}1)_\varepsilon$ beam illustrating the first epsilon variant in (a).

(f) Dark field image of the $(1\bar{1}1)$ twin variant with $(1\bar{1}\bar{1})_T$ twin beam.

(g) Dark field image of the (111) ε' variant with the $(10\bar{1}1)_{\varepsilon'}$ beam from the $[0\bar{1}11]_{\varepsilon'}$ orientation observed in a selected area diffraction pattern from region B illustrating the second epsilon variant in (a).

REFERENCES

1. A. R. Troiano, Trans. ASM, Vol. 52, 1960, p. 52.

2. A. S. Tetelman and H. J. McEvily, Jr., Fracture of Structural Materials, Wiley, 1967.

3. P. Cotterill, The Hydrogen Embrittlement of Metals, Progress in Materials Science, Pergamon Press, New York, Vol. 9, 1961, p. 205.

4. A. R. Elsea and E. E. Flecther, DMIC Report, 196, Battelle Mem. Inst., January 1964.

5. I. M. Bernstein, Mater. Sci. Engin., Vol. 6, 1970, P. 1.

6. G. G. Hancock and H. H. Johnson, Trans. Met. Soc. AIME, Vol. 235, 1966, p. 513.

7. D. P. Williams and H. G. Nelson. Met. Trans., Vol. 1, 1970, p. 63.

8. R. J. Walter, R. P. Jewett and W. T. Chandler, Mater. Sci. Engin., Vol. 5, 1970, p. 98.

9. R. B. Benson, Jr., R. K. Dann and L. W. Roberts, Jr., Trans. Met. Soc. AIME. Vol. 242, 1968, p. 2199.

10. J. A. Harris and M. E. Van Wanderham, Pratt Whitney Aircraft Report FR-4566 (Access No. N71-33728), 1971.

11. R. R. Vandervoort, Met. Eng. Quart., Vol. 12, 1972, p. 10.

12. M. R. Louthan, Jr., G. R. Caskey, Jr., J. A. Donovan and D. E. Rawl, Jr., Mater. Sci. Eng., Vol. 10, 1972, p. 357.

13. H. G. Nelson, NASA Technical Note, NASA TN D-6691, 1972.

14. A. W. Thompson, to be published in Met. Trans.

15. M. B. Whiteman and A. R. Troiano, Corrosion, Vol. 21, 1965, p. 53.

16. M. L. Holzworth, Corrosion, Vol. 25, 1969, p. 107.

17. R. Lagneborg, JISI, Vol. 207, 1969, p. 363.

18. J. Burke, M. L. Mehta, R. Narayan, L'Hydrogrogène dans les Métaux, 1972, p. 149.

19. J. P. Fidelle, J. Legrand and C. Couderc, TMS Paper No. F-11-8 of Met. Soc. of AIME, New York.

20. J. Legrand, M. Caput, C. Couderc, R. Broudeur, J. P. Fidelle, Mémoires Scientifiques Rev. Metallurg., Vol. 68, 1971, p. 861.

21. C. H. White and R. W. K. Honeycombe, JISI, Vol. 200, 1962, p. 457.

22. K. S. Raghavan, A. S. Sastri and M. J. Marcinkowski, Trans. Met. Soc., AIME, Vol. 245, 1969, p. 1569.

23. A. H. Graham and J. L. Youngblood, Met. Trans., Vol. 1, 1970, p. 423.

24. R. B. Benson, Jr., to be published in the proceedings of an international conference entitled Hydrogen In Metals:Effect on Properties, Selection and Design, Seven Springs, Pa., Sept. 1973.

25. R. J. Magone, D. B. Roach and A. M. Hall, DMIC Report 113, May 1959.

26. R. Lagneborg, Acta. Met., Vol. 12, 1964, p. 823.

27. W. N. Roberts, Trans. Met. Soc. AIME, Vol. 230, 1964, p. 372.

28. B. Cina, Acta Met., Vol. 6, 1958, p. 748.

29. H. M. Otte, Acta. Met., Vol. 5, 1957, p. 514.

30. J. A. Venables, Phil. Mag., Vol. 7, 1962, p. 35.

31. J. F. Breedis and W. D. Robertson, Acta. Met., Vol. 11, 1963, p. 547.

32. J. Dash and H. M. Otte, Acta. Met., Vol. 11, 1963, p. 1169.

33. A. R. Troiano and F. T. McGuire, Trans. ASM, Vol. 31, 1943, p. 340.

34. H. Schumann, Arch. Eisenh., Vol. 38, 1967, p. 647.

35. A. Holden, J. D. Bolton and E. R. Petty, JISI, Vol. 209, 1971, p. 721.

36. R. A. McCoy, W. W. Gerberich, V. F. Zackay, Met. Trans., Vol. 1, 1970, p. 2031.

37. R. R. Vandervoort, A. W. Ruotola and E. L. Raymond, Met. Trans., Vol. 4, 1973, p. 893.

38. R. A. McCoy and W. W. Gerberich, Met. Trans. , Vol. 4, 1973, p. 539.

39. R. A. McCoy, Ph.D. thesis, University of California, Berkeley, 1971: To be published in the proceedings of an international conference entitled Hydrogen in Metals: Effect on Properties, Selection, and Design, Seven Springs, Pa., Sept 1973.

40. J. D. Bolton and E. R. Petty, J. Met. Sci, Vol. 5, 1971, p. 166.

41. R. L. Grunes, C. D'Antonio and K. Mukherjee, Mater. Sci. Engin., Vol. 9, 1972, p. 1.

42. Z. Nishiyama, Metal Phys., Vol. 7, 1961, p. 107.

43. J. D. Defilippi, K. G. Brickner, and E. M. Gilbert, Trans. Met. Soc. AIME, Vol. 245, 1969, p. 2141.

44. W. F. Brown, Jr. and J. E. Srawley, Plane Strain Crack Toughness Testing of High Strength Metallic Materials, ASTM Special Technical Publications 410, 1966, p. 12.

45. D. J. Drobnjak and J. Gordon Parr, Met. Trans., Vol. 1, 1970, p. 759.

46. H. G. Nelson, D. P. Williams and A. S. Tetelman, Met. Trans., Vol. 2, 1971, p. 953.

47. H. G. Nelson, Testing for Hydrogen Embrittlement: Primary and Secondary Influences. ASTM, Special Technical Publication, to be published in 1973.

48. E. E. Fletcher and A. R. Elsea, DMIC Report 219, Battelle Mem. Inst., June 1965.

49. H. G. Nelson and J. E. Stein, NASA Technical Note, NASA TN D-7265, 1973.

50. C. E. Spaeder, Jr., J. C. Majetich and K. G. Brickner, Met. Engin. Quart., Vol. 9. 1964, p. 1.

51. J. W. Christian and P. R. Swann, Alloying Behaviour and Effects in Concentrated Solid Solutions, AIME Metallurgical Society Conference, Vol. 29. p. 105, Gordon and Breach, N. Y., 1965.

52. H. Fujita and S. Ueda, Acta. Met., Vol. 20, 1972, p. 759.

53. J. M. Drapier, P. Viatour, D. Coutsouradis and L. Habraken, Cobalt, No. 49, 1970, p. 171.

54. N. J. Petch. Phil. Mag., Vol. 1, 1956, p. 331.